J. Innovative Eng. Nat. Sci., vol. 4, no. 1, pp. 220-231, 2024.
http://doi.org/10.61112/jiens.1395682

JIENS
Journal of Innovative Engineering and Natural Science
(Yenilikçi Mühendislik ve Doğa Bilimleri Dergisi)
journal homepage: https://jiens.org
Original Paper

Enhancing filtration performance with layered and bimodal nanofiber structures

Ali Toptaş[a,b,c,*], Ali Kılıç[a,c] and Ali Demir[a,c]

[a]*Faculty of Textile Technologies and Design, Istanbul Technical University, 34437, Istanbul, Türkiye.*
[b]*Safranbolu Vocational School, Karabuk University, 78600, Karabuk, Türkiye.*
[c]*TEMAG Labs, Faculty of Textile Technologies and Design, Istanbul Technical University, 34437, Istanbul, Türkiye*

ARTICLE INFO

Article history:
Received 7 Nov 2023
Received in revised form 19 Dec 2023
Accepted 10 Jan 2024

Available online

Keywords:
Bimodal
Air Filter
Meltblown
Electro-Blowing
Corona Discharge

ABSTRACT

Particulate matter (PM) must be removed from the air because it is a serious threat to human health. Micro and/or nanoporous nonwoven fabrics are commonly used to filter these particles. In our study, the filtration performances of nanofibrous mats, which were obtained by combining fibers produced by two different production methods in a layered and bimodal manner, were evaluated. Fibrous layers produced by the meltblown (MB) method were obtained with similar fiber diameters and different thicknesses by different feeding speeds. Bimodal structures obtained by adding fibers with an average diameter of 225 nm produced by the solution blowing (SB) method into fibers with an average diameter of around 800 nm obtained at 1, 5 and 10 rpm screw rotating/feeding speeds had higher filtration performance than the samples without SB nanofibers. Then, among the four samples with an average basis weight of 15 gsm, the sample MB only without (electro-blown nanofiber); the EB sample contains only EB nanofibers; the sample (L) containing 4 gsm EB nanofibers and the 4-layer sample (4L) containing 4 gsm EB nanofibers (138 nm) were compared. The 4L sample had the highest quality factor (0.0353) with a filtration efficiency of 96.01% and a pressure drop of 135 Pa. Although the filtration efficiency increased in all samples with the subsequent corona treatment, the highest value (99.34%) was obtained from the 4L sample.

I. INTRODUCTION

Air pollution is a major global problem that has serious impacts on health, environment, and quality of life [1]. Increasing industrial activities, vehicle exhausts, energy production and other human activities negatively affect the air quality [2]. Pollutants, especially those containing fine particulate matter (PM), are among the factors that increase the risk of respiratory diseases, cardiovascular diseases and even death [3].

In this context, the air filtration systems stand out as an important way to provide clean air at indoors and outdoors [4]. Traditional air filters are effective at circulating clean air by capturing and trapping the airborne pollutants [5]. However, the need for higher performance filtering technologies is increasing to improve air quality and protect our health [6].

Meltblowing (MB) and electro-blowing (EB) methods are two basic methods that are effective in the production of micron and nanometer sized fibers [7, 8]. The MB method involves melting thermoplastic polymers and blowing them at high speed to obtain thin fibers. On the other hand, the EB method involves the formation of nanofibers by diluting the polymer solution under the influence of electrostatic and compressed air forces [9]. While either method alone can produce effective fibers, the potential of the combination of these two methods to achieve more effective results in air filtration has recently been investigated.

*Corresponding author. Tel.: +90-541-286-7827; e-mail: alitoptas@karabuk.edu.tr

The quality factor that determines the effectiveness of a filter mat gives high results with high filtration efficiency and low pressure drop values [10]. Due to the large pore sizes in the filter mats made of microfibers, filtration efficiency is low, and the pressure drop is also low. In a nanofibrous filter mat, high filtration efficiency is accompanied by high pressure drop. To improve this situation, filter mats obtained from microfibers are charged with an electrostatic charge, resulting in an improvement in filtration efficiency with an additional capture mechanism [11].

A bimodal approach is being studied to obtain low pressure drop values by increasing the filtration efficiency of filter mats. The nanofibers mixed between the microfibers on the surfaces formed by combining micro and nanofibers with bimodal filter mats increase the filtration efficiency by creating new air channels and prevent the pressure drop from increasing [12, 13]. In the study conducted by Lin et al., it was revealed that a bimodal filter showed a high filtration performance (98.43%) when the average fiber diameters were 2.44 and 0.13 μm, reducing the pressure drop up to 56.47 Pa [14]. In another study, Mei et al. prepared polyacrylonitrile (PAN) nanofiber mats consisting of fibers with unimodal and bimodal diameter distributions by electrospinning method and analyzed their quality factors (QFs). Bimodal nanofiber mats exhibited higher QFs than unimodal fiber mats with the same weight average fiber diameter [15].

The aim of this study is to examine the effectiveness of the layered combination of fibers produced by MB and EB methods in air filtration. How the layered fiber combination improves filtration performance, how it helps capture airborne particulate matter and pollutants more effectively, and the advantages this new approach can bring to existing air filtration technologies are the focus of this study.

II. EXPERIMENTAL METHOD / THEORETICAL METHOD

2.1 Materials and Preparation Techniques

Polyvinylidene fluoride (PVDF) powders with a molecular weight of 477,000 g/mol were acquired from Arkema Chemicals under the product name Kynar Flex 2801-00. Polypropylene (PP) granules, featuring a melt flow index (MFI) of 1800 g/10 min, were sourced from TEKNOMELT Co, Turkey. Dimethyl sulfoxide (DMSO) with a purity of 99.8% (Merck) and acetone with a purity of 99.5% (ISOlab) were employed as solvents.

In the initial stage, PVDF solutions with a concentration of 12wt.% were prepared using a mixture of acetone and DMSO in a weight ratio of 30/70. These solutions were subjected to magnetic stirring at a temperature of 70 °C for 8 hours.

To examine the impact of screw speed on the basis weight of the produced meltblown (MB) fibers, we employed dried polypropylene (PP) and conducted the meltblown fiber production at varying screw speeds: 1, 5, and 10 rpm. Throughout the production process, we maintained a die-to-collector distance of 25 cm, a mold temperature of 275 °C, a hot air pressure of 3 bar, and a compressed air temperature of 350 °C.

An electro-blowing (EB) system, specifically the Aerospinner from Areka Ltd., was used to produce the nanofibrous mats. This EB system, shown in Figure 1, comprised several components: a pressurized air tank linked to a regulator, a high-voltage power supply, a syringe pump, a co-axial spinning nozzle positioned on a homogenizing shaft to ensure even fiber accumulation, and an injector. To collect the nanofibers, a vacuum-

assisted rotating collector with a surface area of 30 × 20 cm was employed. The all-EB samples were generated with a feed rate of 10 mL/h, an air pressure of 1 bar, and an electric voltage of 30 kV, maintaining 30 cm between the collector nozzle and the source.

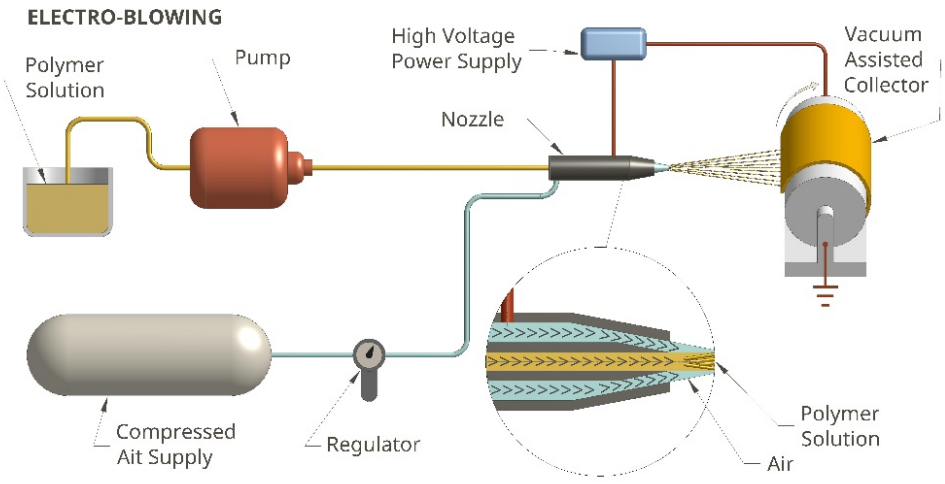

Figure 1. Electro-blowing system [1]

In the case of solution-blowing (SB), a similar system as depicted in Figure 1 was used, without the need for a power supply. SB nanofibers were produced from 12 wt.% PVDF solution with a solution feed rate of 10 mL/h at 2-bar air pressure. To determine the production times for both EB and SB nanofiber mats, accounting for their basis weight, the following Equation 1 was employed:

$$t = \frac{60 * BW * A}{FR * C} \quad (1)$$

Where, BW is basis weight, A is area of the collector, FR is feeding rate and C is concentration of the polymer solution.

2.2. Preparation of Bimodal Filter Samples

The schematization of four different samples explanations produced within the scope of the study was given in Figure 2. The black lines in the image represent the fibers produced by the MB method, the yellow lines represent the fibers obtained by the SB method, and the red lines represent the fibers produced by the EB method. The weights of all samples were adjusted to an average of 15 gsm (grams per square meter). The 4L sample contains approximately 11 gsm bimodal MB-SB layer and 4 gsm layer of EB nanofibers. However, this MB-SB mat and EB mat were brought together in 4 layers, allowing the EB nanofibers to be dispersed into the structure. In sample L, 4 gsm EB nanofibers were collected as a single layer on the 10.34 gsm MB-SB layer. The

MB sample was produced from 15.32 gsm MB fibers, and EB sample was produced from only EB nanofibers with a weight of 15 gsm.

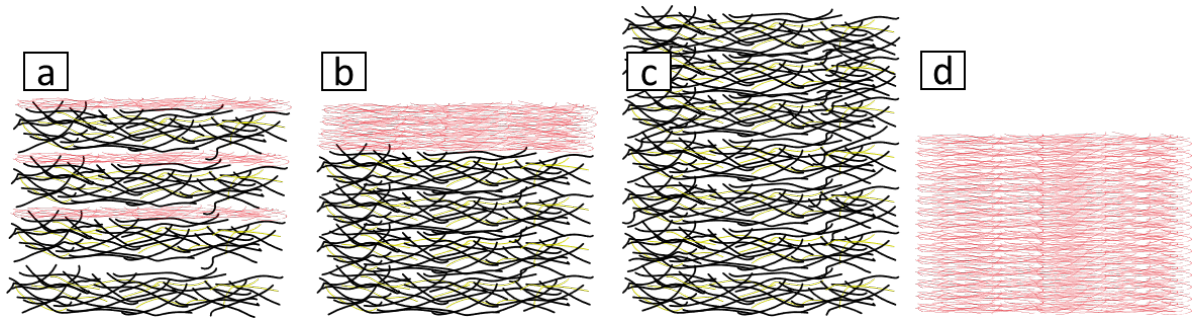

Figure 2. Schematic representation of the produced samples a) 4L, b) L, c) MB and d) EB

To produce MB-SB bimodal layers, the system schematized in Figure 3 was used. In this system, two SB nozzles were used, which produce simultaneously with the MB production method and were placed on both sides of the MB device. Therefore, MB and SB fibers were collected homogeneously on the same surface.

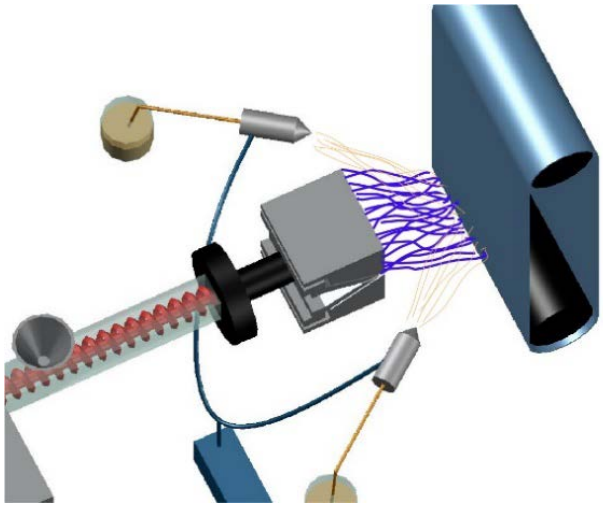

Figure 3. MB-SB bimodal production system

The fibrous structures' appearances were assessed via scanning electron microscopy (SEM), specifically using the TESCAN VEGA 3 model. To facilitate the conductivity, a thin layer of gold/palladium, with 10 nm in thickness was applied to the samples prior to SEM analysis. Average fiber diameters (AFD) and their standard deviations were determined from SEM images, magnified at 5kx times, utilizing the ImageJ software. To gauge the filtration performance of the samples in terms of pressure drop (ΔP) and filtration efficiency (η), an automatic filter test device (model 8130A, TSI Inc.) was employed. For this evaluation, solid salt particles, with an approximate diameter of 0.26 ± 0.07 μm, were generated from a 2 wt.% NaCl solution. The nanofiber mats, featuring an effective area of 100 cm², were subjected to testing against NaCl aerosols at a surface velocity of

15.83 cm/s. The results obtained according to ISO 16890 standards provide ePM1 level (>95% against 0.3–1 μm dust). The filtration efficiency (η) was calculated using Equation 2.

$$\eta = 1 - C_{down}/C_{up} \tag{2}$$

In this context, where "C_{down}" represents downstream particle concentration and "C_{up}" represents upstream particle concentration, the mathematical expression for the quality factor (QF), designed to evaluate the filter sample's quality by taking into account both filtration efficiency and ΔP, is defined by Equation 3:

$$QF = -\frac{ln(1-\eta)}{\Delta P} \tag{3}$$

III. RESULTS AND DISCUSSIONS

3.1. Morphology

In the MB process, screw speed controls the amount of melt fed, and higher screw speeds result in a greater amount of fiber produced per unit time. In this study, MB fibers were produced using PP at different screw speeds of 1, 5 and 10 rpm. The thickness and basis weight values of these samples are presented in Figure 4. The thinnest and lightest sample was obtained with a basis weight of 2.5 gsm and a screw speed of 1 rpm. As the screw speed increased, both the thickness and weight of the fibrous mats increased.

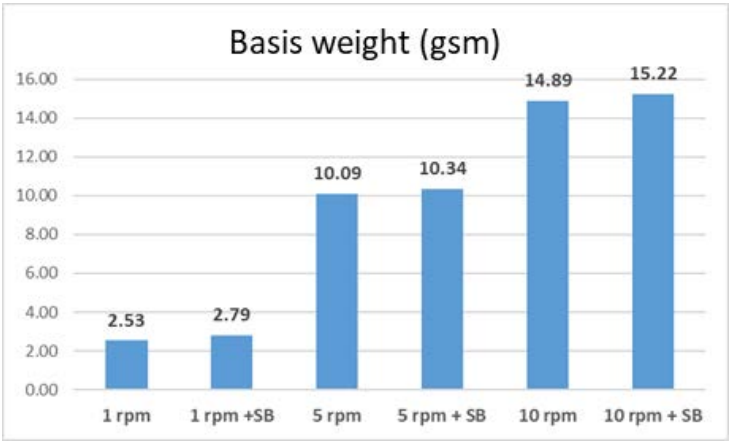

Figure 4. Basis weigths of the MB and MB-SB samples

Figure 4 shows the proportions of nanofibers produced with the SB nozzles added to the MB system. While this ratio is highest at 1 rpm, as the MB production rate increases, the amount of SB nanofibers in the structure decreases.

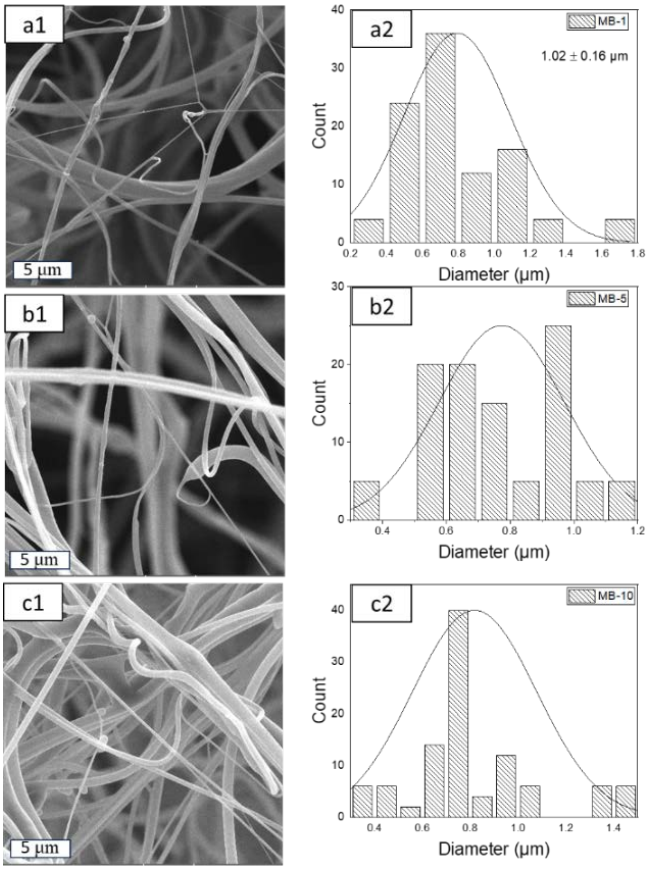

Figure 5. SEM images and AFD diagrams of the samples

SEM images of MB-SB samples and EB samples were given in Figure 5. According to Figure 5a2-c2, the avarage diameters of the fibers obtained by the MB method were measured as 775 ± 245 nm, 799 ± 274 nm and 838 ± 286 nm, and no significant change was observed in terms of fiber diameters between the samples. The diameter of the nanofibers produced using the SB method was measured as 225 nm. The dromedary fiber diameter diagram given in Figure 6 shows that MB and SB nanofibers have bimodal distribution in the same structure.

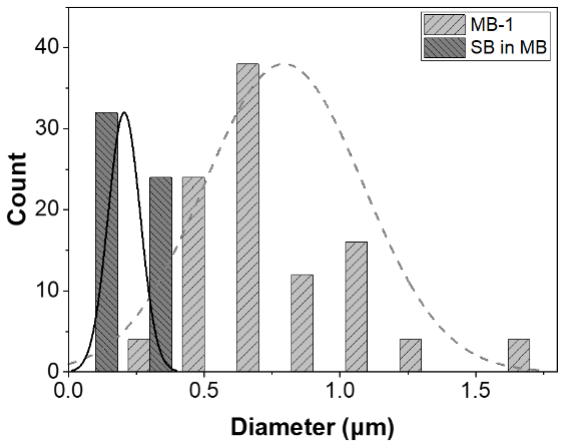

Figure 6. AFD diagram of the MB-SB bimodal sample

The MB method had the ability to produce a larger amount of fiber per unit time as it ensures that the molten polymer completely turned into fiber. On the other hand, the advantage of solution-based methods was that the fiber diameters are thinner than the fibers obtained by the MB method. In this study, the AFD_MB/AFD_EB ratio was approximately 5 times. In addition, reducing the solution concentration and adding electric field in solution-based productions are very important factors in thinning the fiber diameter. The 39% thinning (225 to 138 nm) of fibers obtained with the EB method compared to the fibers obtained with the SB method proves this.

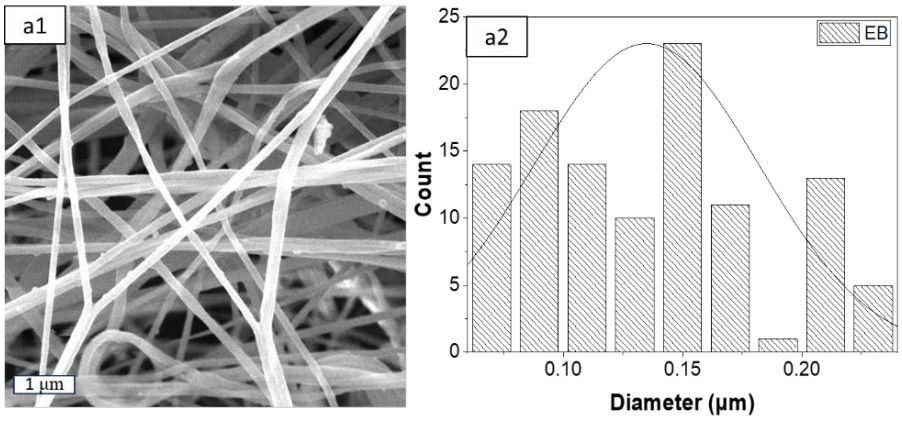

Figure 7. Sem image and AFD diagram of the EB sample

Figure 7 shows SEM images and fiber diameter diagrams of EB nanofibers. The average diameter of the fibers of this sample, produced in the presence of electric field and compressed air, was 138 ± 43 nm. The absence of droplets in the sample indicates that the selected production parameters were in optimum conditions.

3.2. Filtration Performance

The filtration efficiency and pressure drop values of six samples produced only with the MB method and with the addition of SB nozzles in addition to the MB method were given in Table 1. It was observed that the filtration efficiency of bimodal nanofibrous mats obtained by adding SB nanofibers into MB samples increased. Depending on the increase in weight of MB-SB samples, the highest filtration efficiency values were obtained in the 10 rpm sample. In addition to increased filtration efficiency, the highest quality factor was obtained in the 10 rpm sample, although there was also an increase in pressure drop. In addition, when each sample was evaluated according to whether or not the addition of SB nanofibers was present, there was a significant improvement in filtration efficiency and pressure drop with the addition of SB nanofibers.

Table 1. Filtration efficiencies and pressure drop values of the MB samples

Samples	Efficiency (%)	Pressure Drop (Pa)
1 rpm MB	31.65	45
1 rpm MB + SB	39.54	47
5 rpm MB	45.97	71
5 rpm MB + SB	63.32	73
10 rpm MB	75.56	85
10 rpm MB + SB	83.74	88

The filtration efficiency and pressure drop values of 4L, L and MB-SB and EB samples are given in Figure 6. When the filtration efficiency and pressure drop graphs of MB samples with a weight of 4L, L and 15 gsm are examined in Figure 6a, it is seen that the EB nanofibers included in the structure significantly improve the filtration efficiency. 4L and L samples showed better performance than MB-SB sample with higher filtration efficiency and quality factor values. On the other hand, when samples 4L and L were examined separately, it was seen that these two samples contain the same amount of both MB and EB fibers in their structures. In the 4L sample, the distribution of EB nanofibers in 4 layers within the structure caused a significant improvement in pressure drop while providing a low improvement in filtration efficiency. This was due to the small pore sizes created by thin nanofibers. While these pores provided high filtration efficiency by capturing particles, they also quickly became clogged due to the captured particles, causing an increase in pressure drop. However, the inclusion of EB nanofibers in the structure in 4 layers rather than a single layer caused the particles to be retained throughout the structure by surface filtration and to show high filtration performance by providing a lower pressure drop. In addition, the filtration efficiency value was highest in the sample consisting only of EB nanofibers, thanks to the small pore sizes created by the thin fibers. However, due to the decrease in pore sizes and rapidly filling pores, the pressure drop value was accordingly highest. This showed that filtration efficiency and pressure drop were low in the MB sample, which consisted only of thick fibers. The filtration efficiency value and pressure drop values were highest in the EB sample, which consisted only of thin nanofibers. However, in the 4L sample obtained within the scope of the study and brought together with an appropriate configuration, the filtration efficiency was high while the pressure drop value decreased. This is the most important criterion expected from an effective filter.

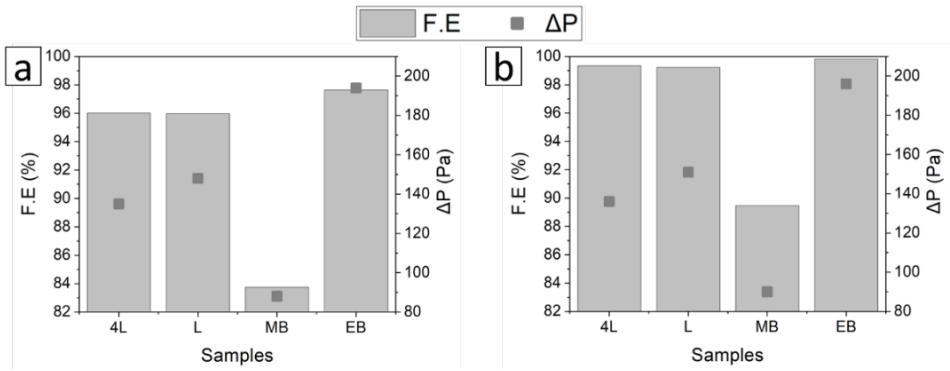

Figure 8. Filtration efficiencies and Pressure drop values of the 4L, L and MB, and EB samples

Figure 8b shows the graph of filtration efficiency and pressure drop after the corona discharge process applied to the samples. An improvement in filtration efficiency was observed in all samples with corona treatment. The sample with the highest filtration efficiency, the 4L sample, was the best sample with a filtration efficiency of 99.18% and a pressure drop of 136 Pa.

Table 2 shows the filtration efficiency and pressure drop values of all samples produced, after corona and after 1 month. Although a decrease in filtration efficiency was observed in all samples after 1 month, the decrease in the 4L sample was the least. The 4L sample showed the highest value with 98.16% filtration efficiency even after 1 month.

Table 2. Filtration efficiencies and pressure drop values of the samples

Sample	As Produced		After Corona		1 M Aged	
	F.E (%)	ΔP (Pa)	F.E (%)	ΔP (Pa)	F.E (%)	ΔP (Pa)
4L	96.01	135	99.34	136	98.16	135
L	95.96	148	99.23	151	97.29	151
MB	83.74	88	89.47	90	85.07	88
EB	97.63	194	99.81	196	98.28	196

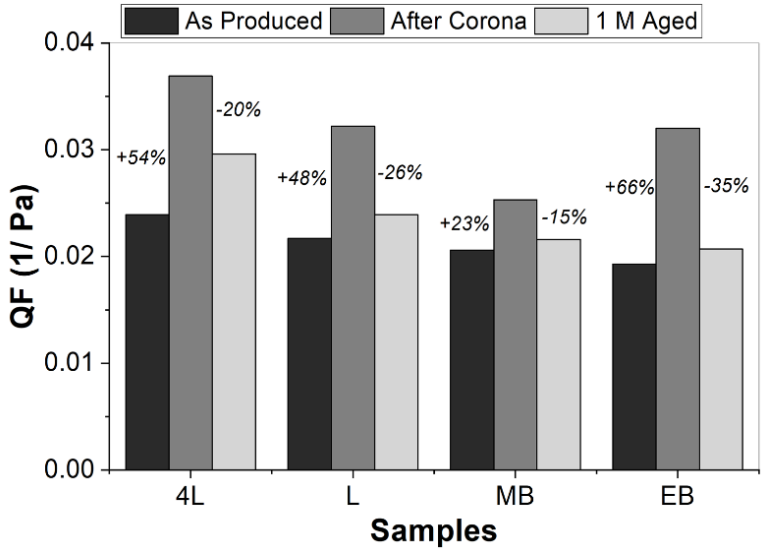

Figure 9. Quality factors of the 4L, L and MB-SB samples

In Figure 9, the values and change rates of quality factors of all samples after production, after corona and after 1 month were given. When the values were examined, the sample that best preserved the efficiency increased by the corona treatment even after 1 month was the 4L sample. This can be explained by the fact that PVDF nanofibers remain in the layered structure and maintain their electrostatic charge because of not interacting with the moisture in the air.

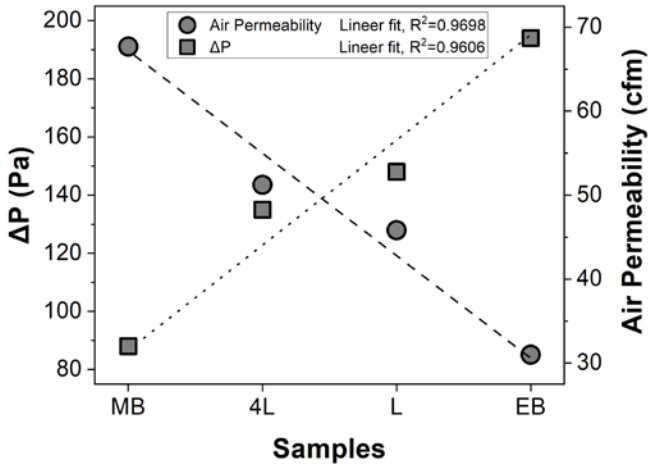

Figure 10. Pressure drop values - Air permeability diagram of the samples

Air permeability is a measure of porosity/space size in fibrous mats, with higher values indicating greater porosity/larger pore sizes. In filtration tests, higher air permeability in samples means lower ΔP. Our samples exhibited a fairly consistent linear behavior in terms of both air permeability and ΔP. When the 4L and L samples are examined, although the total basis weight of the samples does not change according to the number of layers, the multilayer structure consisting of fibers of different sizes distributed throughout the cross-section of the filter creates interlayer channels for air passage. As a result, as the number of layers increases in the dual-mode multilayer structure, air permeability increases and accordingly the pressure drop (ΔP) decreases. The air permeability value was lowest in the EB sample consisting of the thinnest nanofibers, which can be explained by the small pore sizes created by the thin nanofibers making it difficult for air to pass through. The excellent agreement between air permeability and ΔP confirmed that the approach of using layers of different thicknesses composed of fibers of different sizes was an effective strategy to increase filtration performance.

Table 3: Comparison of filter samples obtained from bimodal fibers

Materials	Production method	Filtration efficiency (%)	Pressure Drop (Pa)	References
PP-PVDF	Meltblowing and Electro-blowing	99.340	136	This study
		99.230	151	This study
Zein	Electrospinning	97.010	38	[14]
PAN	Electrospinning	99.936	220	[15]
PLA	Electrospinning	99.440	163	[16]
PA6	Solution blowing	99.891	168	[12]

When we investigate the table where information about filter samples obtained from bimodal fibers is examined, we can see samples obtained from different polymers and different production methods. High filtration efficiencies were obtained in studies using different polymers and different production methods. Increasing filtration efficiency was generally followed by increased pressure drop. When studies in the literature are examined, the 4L sample obtained from PP and PVDF polymers has an outstanding value with 99.34% filtration efficiency and 136 PA pressure drop.

Bimodal filter structures, showcasing impressive practical results, have drawn attention in a variety of potential real-world applications. These structures, known for their ability to capture a wide spectrum of particles by combining fibers of different sizes, can be particularly effective in air filtration, ranging from harmful nanoparticles to micrometer-sized particles. Thanks to these features, bimodal filters have the potential to address a range of applications, such as improving urban air quality, controlling particulate matter emissions from industrial waste, and reducing respiratory diseases.

Furthermore, bimodal filter structures have broad potential in various sectors, from the energy industry to the automotive sector. These filters, with their different-sized fibers, can better respond to specific needs in certain applications. For example, in energy production facilities, they might effectively filter harmful particles in combustion byproducts. In the automotive industry, bimodal filters could play an effective role in reducing emissions of nano-sized particles in exhaust gases.

Therefore, bimodal filter structures represent a wide potential for addressing practical issues such as improving environmental quality and controlling harmful emissions in industrial processes. Future studies could focus on

further optimizing the characteristics of these filters to tailor them for specific applications, contributing to a healthier environment and sustainable industrial practices.

Bimodal filter structures represent an area with significant potential for future research. These structures offer the potential to increase efficiency, especially in air filtration and similar applications, with the combination of materials with different fiber sizes. Future studies may focus on exploring optimized designs, material combinations, and fabrication methods of bimodal filters. This can be critical for improving the effectiveness of filters against a wider particle size distribution, optimizing energy efficiency, and ensuring long-lasting performance. Additionally, advances in nanotechnology and materials science may offer new opportunities to further improve the properties of bimodal filters. Future research in this direction may have the potential to provide more effective and sustainable solutions in air quality management and industrial applications.

IV. CONCLUSIONS

In our study, where we aimed to show the improvement in filtration efficiency and pressure drop values provided by bimodal structures, it was observed that filtration efficiency improved by adding SB nanofibers to the structure of MB filter mats. In addition, in 4 different samples (L, 4L, MB and EB) with the same basis weight (15 gsm), the addition of nanofibers to the structure and the distribution of nanofibers into the structure by layered work both increased the filtration efficiency (99.34%) and caused an improvement in pressure drop (136 Pa). The results show that bimodal structures can be structures with high quality factor and long life in the filtering process.

ACKNOWLEDGMENT

The authors would like to thank Areka Filtration Technologies LLC, provider of the electroblowing system AeroSpinner E1.0.

REFERENCES

[1] Kaur R, Pandey P (2021) Air Pollution, Climate Change, and Human Health in Indian Cities: A Brief Review. Front in Sustainable Cities 705131-3. https://doi.org/10.3389/frsc.2021.705131
[2] Khajavi R, Bahadoran MMS, Bahador A (2012) Removal of microbes and air pollutants passing through nonwoven polypropylene filters by activated carbon and nanosilver colloidal layers. J Ind Text 42:219-230. https://doi.org/10.1177/1528083711434653
[3] Schwartz J, Laden F, Zanobetti A (2002) The concentration-response relation between PM(2.5) and daily deaths. Environ Health Perspect 110:1025–1029. https://doi.org/10.1289/ehp.021101025
[4] Shoeib M, Harner T, Wilford BH, Jones KC, Zhu J (2005) Perfluorinated Sulfonamides in Indoor and Outdoor Air and Indoor Dust: Occurrence, Partitioning, and Human Exposure. Environ Sci Technol 39:6599–6606. https://doi.org/10.1021/es048340y
[5] Hyttinen M, Pasanen P, Kalliokoski P (2001) Adsorption and desorption of selected VOCs in dust collected on air filters. Atmos Environ 35:5709-5716. https://doi.org/10.1016/S1352-2310(01)00376-4
[6] Kilic A, Shim E, Pourdeyhimi B (2015) Electrostatic Capture Efficiency Enhancement of Polypropylene Electret Filters with Barium Titanate. Aerosol Sci Technol 49:666–673. https://doi.org/10.1080/02786826.2015.1061649
[7] Erben J, Jencova V, Chvojka J, Blazkova L, Strnadova K, Modrak M, et al. (2016). The combination of meltblown technology and electrospinning – The influence of the ratio of micro and nanofibers on cell viability. Mater Lett 173:153–157. https://doi.org/10.1016/j.matlet.2016.02.147

[8] Eticha A, Toptaş A, Akgül Y, Kılıç A (2023) Electrically assisted solution blow spinning of PVDF/TPU nanofibrous mats for air filtration applications. Turk J Chem 47:47–53. https://doi.org/10.55730/1300-0527.3515
[9] Wang X, Um IC, Fang D, Okamoto A, Hsiao BS, Chu B (2005) Formation of water-resistant hyaluronic acid nanofibers by blowing-assisted electro-spinning and non-toxic post treatments. Polym 46:4853-4867. https://doi.org/10.1016/j.polymer.2005.03.058
[10] Choi HJ, Kumita M, Hayashi S, Yuasa H, Kamiyama M, Seto T, et al. (2017) Filtration Properties of Nanofiber/Microfiber Mixed Filter and Prediction of its Performance. Aerosol Air Qual Res 17:1052–1062. doi: 10.4209/aaqr.2016.06.0256
[11] Kilic A, Russell S, Shim E, Pourdeyhimi B (2017) 4- The charging and stability of electret filters. in: P.J. Brown, C.L. Cox (Eds.), Fibrous Filter Media, Woodhead Publishing, pp. 95–121. https://doi.org/10.1016/B978-0-08-100573-6.00025-3
[12] Gungor M, Selcuk S, Toptas A, Kilic A (2022) Aerosol Filtration Performance of Solution Blown PA6 Webs with Bimodal Fiber Distribution. ACS Omega 7:46602–46612. https://doi.org/10.1021/acsomega.2c05449
[13] Toptas A, Calisir DM, Kilic A (2023) Production of Ultrafine PVDF Nanofiber-/Nanonet-Based Air Filters via the Electroblowing Technique by Employing PEG as a Pore-Forming Agent. ACS Omega 41:38557–38565. https://doi.org/10.1021/acsomega.3c05509
[14] Lin S, Fu X, Luo M, Zhong WH (2022) Tailoring bimodal protein fabrics for enhanced air filtration performance. Sep Purif Technol 290:120913. https://doi.org/10.1016/j.seppur.2022.120913
[15] Mei Y, Wang Z, Li X (2013) Improving filtration performance of electrospun nanofiber mats by a bimodal method. J Appl Polym Sci 128:1089–1094. https://doi.org/10.1002/app.38296
[16] Lin M, Shen J, Wang B, Chen Y, Zhang C, Qi H (2023) Preparation of fluffy bimodal conjugated electrospun poly(lactic acid) air filters with low pressure drop. RSC Adv 13:30680–30689. https://doi.org/10.1039/D3RA05969C